



Deposited via The University of Sheffield.

White Rose Research Online URL for this paper:

<https://eprints.whiterose.ac.uk/id/eprint/106327/>

Version: Accepted Version

Article:

Clarke, M., Volpe, G., Sheriff, L. et al. (2017) Transcriptional regulation of SPROUTY 2 by MYB influences myeloid cell proliferation and stem cell properties by enhancing responsiveness to IL-3. *Leukemia*, 31. pp. 957-966. ISSN: 0887-6924

<https://doi.org/10.1038/leu.2016.289>

Reuse

Items deposited in White Rose Research Online are protected by copyright, with all rights reserved unless indicated otherwise. They may be downloaded and/or printed for private study, or other acts as permitted by national copyright laws. The publisher or other rights holders may allow further reproduction and re-use of the full text version. This is indicated by the licence information on the White Rose Research Online record for the item.

Takedown

If you consider content in White Rose Research Online to be in breach of UK law, please notify us by emailing eprints@whiterose.ac.uk including the URL of the record and the reason for the withdrawal request.

1 **Transcriptional regulation of SPROUTY 2 by MYB**
2 **influences myeloid cell proliferation and stem cell**
3 **properties by enhancing responsiveness to IL-3**

4

5 Mary Clarke, Giacomo Volpe, Lozan Sheriff, David Walton, Carl Ward, Wenbin Wei,
6 Stephanie Dumon¹, Paloma García¹ and Jon Frampton^{1,2}

7

8 Institute of Cancer and Genomic Sciences, College of Medical and Dental Sciences,
9 University of Birmingham, Edgbaston, Birmingham B15 2TT, UK

10

11 ¹ Co-senior authors

12 ² Corresponding author, Email j.frampton@bham.ac.uk

13

14 Keywords: MYB / myeloproliferative neoplasm / hematopoietic stem cells / IL-3 signaling

15 Running title: MYB modulates myeloproliferation through IL-3 signaling

16

17 Word count: 3988

18

19 **ABSTRACT**

20 Myeloproliferative neoplasms (MPN), which overproduce blood cells in the bone marrow,
21 have recently been linked with a genetically determined decrease in expression of the MYB
22 transcription factor. Here, we use a mouse MYB knockdown model with an MPN-like
23 phenotype to show how lower levels of MYB lead to stem cell characteristics in myeloid
24 progenitors. The altered progenitor properties feature elevated cytokine responsiveness,
25 especially to IL-3, which results from increased receptor expression and increased MAPK
26 activity leading to enhanced phosphorylation of a key regulator of protein synthesis,
27 ribosomal protein S6. MYB acts on MAPK signaling by directly regulating transcription of the
28 gene encoding the negative modulator SPRY2. This mechanistic insight points to pathways
29 that might be targeted therapeutically in MPN.

30

31 INTRODUCTION

32 Myeloproliferative neoplasms (MPN) are a heterogeneous group of hematological disorders
33 characterized by over production of one or more myeloid lineages that can lead to the
34 evolution of myeloid leukemia. Several genetic lesions have been described that lead to the
35 evolution of MPN, exemplified by JAK2^{V617F} and mutations in calreticulin (CALR) and the
36 thrombopoietin receptor, MPL (1-3). Although the JAK2^{V617F} mutation is associated with
37 more than 95% of polycythemia vera (PV) and 50-60% of essential thrombocythemia (ET)
38 and primary myelofibrosis (PMF) there are increasing reports of JAK2^{V617F}-negative MPN
39 and indeed cases of MPN that are negative for mutations in JAK, MPL and CALR. Recently,
40 a study on MPN patients identified potential mutations that predispose to and drive the
41 development of MPN (4). One of the polymorphisms identified was rs9376092, which is
42 found 75 kb telomeric of the gene encoding the oncogenic transcription factor MYB.
43 Interestingly, this risk allele is associated with reduced *MYB* RNA expression in both normal
44 myeloid cells and JAK2^{V617F} mutant BFU-E from ET patients compared to the equivalent wild
45 type cells.

46 Studies on mouse models have suggested that decreased activity of MYB can lead to
47 phenotypes that reflect at least some aspects of MPN (5, 6). We showed that reduced levels
48 of MYB in mice homozygous for a knockdown allele (*MYB*^{KD/KD}) result in a MPN-like disorder
49 resembling human ET, which is underpinned by a KIT⁺CD11b⁺Lin^{low} (K11bL) cell that is stem
50 cell like (5).

51 In this study we have sought to understand how a lower level of MYB in myeloid progenitors
52 leads to a gain of stem cell characteristics and the MPN-like phenotype, and thereby shed
53 light on the observed effect of lower MYB levels on the development of human MPN. We
54 further characterize *MYB*^{KD/KD} K11bL cells and show that enhanced IL-3 signaling is a key
55 consequence of lower MYB activity. The enhanced response to IL-3 is primarily the result of
56 an increase in MAPK signalling. We demonstrate that these changes arise at least in part

57 from reduced activity of the signaling modulator SPROUTY2, the gene expression of which
58 is directly regulated by MYB.

59

60 **MATERIALS AND METHODS**

61 **Sources of haematological tissues**

62 Animal experiments were carried out in accordance with UK legislation. Human umbilical
63 cord blood samples were collected with informed written consent and was approved by the
64 NRES Committee North West – Haydock.

65 **Flow cytometry and cell sorting**

66 This was performed as previously described (7). All mouse antibodies are listed in
67 **Supplementary Table 1**. For human CD34+ cell sorting, we used anti-CD34 PE (BD
68 Biosciences).

69 **Phospho-flow analysis**

70 K11bL cells were cultured in serum-free medium for 90 min, and then stimulated with
71 20ng/ml IL-3 for 15 min at 37°C. Phospho-flow was performed as previously described (8).
72 Antibodies were PE-conjugated (Cell Signalling Technology). For inhibition experiments,
73 cells were pre-treated with either 1µM Rapamycin or 10µM U0126 (Sigma) in serum-free
74 media at 37°C for 1 hour.

75 **Engraftment potential of stem cells**

76 Cell transplantation experiments were carried as previously described (5) with 10 000 K11bL
77 (CD45.2/CD45.2) cells injected together with 3×10^5 reference (CD45.1/CD45.2) bone
78 marrow cells.

79 **Homing assays**

80 Sorted K11bL cells were labeled with 0.3 mg/ml Xenolight DiR (Caliper Life Sciences) for 30
81 min at 37°C. Cells were washed and re-suspended in 150µl of PBS, and injected via the tail

82 vein into lethally irradiate hosts (B6:SJL). Details of IVIS imaging conditions can be found in
83 Supplementary Information.

84 **Transfection and cell culture**

85 Human CD34⁺ were sorted and transfected using the 4D-Nucleofector system (Lonza) with
86 FAM-labeled siRNAs (**Supplementary Table 2**). Following transfection, CD34⁺ cells were
87 cultured for 24 hours in RPMI supplemented with 10% FBS, 50ng/ml SCF, 10ng/ml IL3 and
88 20ng/ml IL6. After 24 hours cells were plated in complete methylcellulose (Methocult GF
89 H84435). Colony morphology and number were assessed between 7-14 days.

90 **Transduction of bone marrow cells**

91 Lentiviruses (Origene) expressing shRNA *SPRY2* (TG515588) or *Ii3ra* (TG516353) or
92 *SPRY2* ORF together with GFP, were generated as described (9). Bone marrow or K11bL
93 cells were cultured in the presence of 3µg/ml Polybrene (Sigma) with lentivirus at an MOI of
94 10. Cells were cultured for 4 hours, washed and either injected into lethally irradiated mice or
95 further cultured for 20 hours. Infection efficiency was assessed based on GFP expression.

96 **Gene expression analysis**

97 Affymetrix Mouse Gene 1.0 ST array analysis was performed on K11bL cells. The GEO
98 accession number for the data deposited is GSE74140. Further detail can be found in
99 Supplementary Information. Quantitative PCR was performed as previously described (5).
100 TaqMan PCR primers (Applied Biosystems) and primer sequences are listed in
101 **Supplementary Table 3**.

102 **X-ChIP analysis**

103 X-ChIP assays were performed as previously described (10) using antibodies from Santa
104 Cruz Biotechnology and anti-MYB antibody from Merck Millipore. Primers for detection of
105 MYB binding to the *SPRY2* and *DUSP6* genes are listed in **Supplementary Table 4**.

106 **Statistical analysis**

107 Significance of data sets was assessed using two-tailed unpaired Student's t-test with
108 significance set at $p < 0.05$.

109

110 RESULTS

111 ***MYB*^{KD/KD} K11bL cells exhibit myeloid bias and have stem cell characteristics**

112 When K11bL cells, which are more abundant in *MYB*^{KD/KD} mice compared to *MYB*^{WT/WT}
113 controls (**Figure 1A**), were transplanted into lethally irradiated mice they engrafted
114 significantly, irrespective of whether they were *MYB*^{WT/WT} or *MYB*^{KD/KD} (**Supplementary**
115 **Figure 1A**). However, engrafted *MYB*^{KD/KD} K11bL cells gave rise predominantly in the
116 peripheral blood to CD11b⁺ myelomonocytic cells whereas *MYB*^{WT/WT} K11bL cells largely
117 differentiated into B220⁺ B-lymphoid cells (**Figure 1B**), and all bone marrow K11bL cells
118 derived from *MYB*^{KD/KD} donor cells were positive for CD41 (**Supplementary Figure 1B**).
119 Importantly, when bone marrow isolated from the primary recipients was transplanted into
120 secondary hosts, *MYB*^{WT/WT} K11bL cells failed to support serial engraftment, whereas
121 *MYB*^{KD/KD} cells were able to perpetuate the myeloproliferative phenotype (**Supplementary**
122 **Figure 1C**).

123 We confirmed the *MYB*^{KD/KD} lineage bias of K11bL cells by in vitro colony assay. *MYB*^{KD/KD}
124 cells predominantly formed CFU-M and CFU-M/Mk colonies, failing to produce colonies of
125 granulocytic or erythroid morphology, whereas *MYB*^{WT/WT} K11bL cells were able to undergo
126 a full program of myeloid differentiation (**Supplementary Figure 1D**). Microarray analysis
127 of K11bL cells confirmed the shift from a lymphoid to a myeloid bias, Gene Ontology (GO)
128 analysis showing that compared to *MYB*^{WT/WT} K11bL cells, *MYB*^{KD/KD} cells exhibit higher
129 expression of genes associated with myeloid differentiation, and reduced levels of lymphoid-
130 associated genes (**Supplementary Table 5**).

131 We sought to identify the differences in surface marker and gene expression that might
132 explain the stem cell-like transplantation behaviour of *MYB*^{KD/KD} K11bL cells (**Figure 1Ci and**

133 **Supplementary Figure 1E).** *MYB*^{KD/KD} K11bL cells have higher levels of expression of the
134 integrins CD51 (α_v), CD41 (α IIb) and CD61 (β 3) and the adhesion molecule CD62 (P-
135 selectin). Since *MYB*^{KD/KD} K11bL cells have gained stem cell properties, we analysed the
136 microarray for expression of homing and bone marrow retention molecules together with flow
137 cytometric analysis of some of the key proteins. Analysis of RNA expression data for the
138 GO group “cell chemotaxis” (GO:0060326) revealed an increase in expression of genes
139 associated with homing and invasion of extramedullary sites of hematopoiesis (eg *Ccr1*) and
140 lower levels of genes regulating bone marrow retention (eg *Vcam1*) (**Supplementary Table**
141 **6**). Flow cytometric analysis confirmed the reduction of VCAM1 on the surface of *MYB*^{KD/KD}
142 K11bL cells (**Figure 1Cii and Supplementary Figure 1E**). Consistent with their stem cell
143 characteristics, *MYB*^{KD/KD} K11bL cells have higher levels of SCA1 and CD34, and exhibit a
144 small but significantly higher level of the SLAM marker CD150 ($p \leq 0.01$) (**Figure 1Ciii and**
145 **Supplementary Figure 1E**).

146 ***MYB*^{KD/KD} K11bL cells have an enhanced response to IL-3**

147 Interestingly, analysis of genes in the GO group “cytokine-mediated signaling pathway”
148 (GO:0019221) revealed that a number of cytokine receptor genes are more highly expressed
149 in *MYB*^{KD/KD} K11bL cells compared to the *MYB*^{WT/WT} equivalent. Amongst these genes we
150 identified *CSF2RB* (*IL3RBC*) as being more highly expressed in *MYB*^{KD/KD} K11bL cells (2.25-
151 fold $p = 7 \times 10^{-5}$ **Supplementary Table 7**). This difference, together with that of the other IL-3
152 receptor component *IL3RA*, was confirmed by quantitative PCR (**Figure 2A**).
153 Correspondingly, immunofluorescence analysis showed that the expression of IL3RA
154 (CD123) and CSF2RB (CD131) are greater on *MYB*^{KD/KD} K11bL cells than the *MYB*^{WT/WT}
155 equivalents (**Supplementary Figure 2A**).

156 It is well documented that malignant cells can exhibit a heightened response to growth
157 factors, augmenting their proliferation and survival. Our observations on altered IL-3 receptor
158 expression on *MYB*^{KD/KD} K11bL cells combined with the fate of the cells following
159 transplantation led us to ask if altered responses to IL-3 could be dictating stem cell

160 characteristics. When we plated cells in semi-solid media containing a range of
161 concentrations of IL-3, this revealed that *MYB*^{KD/KD} K11bL cells have a heightened response
162 to the cytokine as manifested by higher colony numbers. This enhancement was significant
163 at all concentrations tested down to 0.02ng/ml ($p \leq 0.05$) (**Figure 2B**). Analysis of colony
164 morphology showed that *MYB*^{WT/WT} K11bL cells yielded colonies containing granulocytes
165 (CFU-G), macrophage (CFU-M), and a mix of both of these cell types (CFU-GM). In
166 contrast, *MYB*^{KD/KD} cells formed mainly CFU-M, which were highly proliferative and gave rise
167 to disperse colonies as well as a few colonies containing both macrophages and
168 megakaryocytes (**Figure 2C**).

169 **IL-3 signaling is critical for *MYB*^{KD/KD} K11bL cell function**

170 To determine how dependent *MYB*^{WT/WT} and *MYB*^{KD/KD} K11bL cells are on signaling through
171 the IL-3 receptor, even in the presence of other growth factors, we used a neutralizing
172 antibody against the IL-3 receptor subunit IL3RB to inhibit the response to IL-3. We
173 observed a marked reduction in colony number from 19 ± 1 to 8 ± 0 ($p = 0.004$) for *MYB*^{KD/KD}
174 K11bL cells, but saw no effect on *MYB*^{WT/WT} cells (**Figure 3A**), suggesting that *MYB*^{KD/KD}
175 K11bL cells are critically dependent on signaling through the IL-3 receptor.

176 Since IL3RB is common to signaling through both the IL-3 and GM-CSF receptors, we
177 wanted directly to assess the effect of knocking down the other IL-3-specific subunit, IL3RA.
178 *MYB*^{KD/KD} K11bL cells were transduced with lentivirus expressing *IL3RA* shRNA and were
179 then transplanted into lethally irradiated mice. Co-expression of GFP from the shRNA vector
180 indicated that we achieved a transduction rate of ~70% (**Figure 3Bi**). Engraftment was
181 apparent after one month, however the proportion of donor cells in the peripheral blood was
182 markedly reduced when IL3RA was knocked down. By 3 months this difference was more
183 evident (**Figure 3Bii**). Interestingly, *MYB*^{KD/KD} donor cells expressing shRNA *IL3RA* had a
184 significantly reduced differentiation towards monocytes ($\text{Gr1}^- \text{CD11b}^+$) compared to control
185 cells ($69 \pm 3\%$ compared to $57 \pm 2\%$, $p \leq 0.01$) and a corresponding increase in differentiation
186 towards granulocytes ($\text{Gr1}^+ \text{CD11b}^+$) (**Supplementary Figure 2B**). Similar to previous

187 observations, the ratio of shRNA control transduced donor $MYB^{KD/KD}$ cells rapidly increased
 188 between 1 and 7 months following transplantation, whereas the cells expressing shRNA
 189 *IL3RA* were maintained at their low engraftment ratio, indicating a necessity for the
 190 expression of IL3RA for engraftment of $MYB^{KD/KD}$ K11bL cells (**Supplementary Figure 2C**).

191 The influence of enhanced IL-3 signaling on engraftment was further examined with respect
 192 to short term migration and homing following transplantation. Following injection of
 193 fluorescently labeled K11bL cells it was evident after one hour that the $MYB^{KD/KD}$ cells have
 194 distinct homing behavior compared to $MYB^{WT/WT}$ K11bL cells, with the predominant signal
 195 emanating from the spleen. Using the IL3RB blocking antibody we then showed that active
 196 signaling through IL3RB is required for the ability of $MYB^{KD/KD}$ K11bL cells to home towards
 197 the spleen as evidenced by a loss of fluorescence signal (9 ± 1 to 0.44 ± 0.2 photon/s $p=0.007$)
 198 when IL3RB was blocked (**Figure 3C and Supplementary Figure 2D**).

199 **Signaling downstream of the IL-3 receptor is enhanced in $MYB^{KD/KD}$ K11bL cells**

200 We used phospho-flow cytometry to determine if the enhanced response of $MYB^{KD/KD}$ K11bL
 201 cells is reflected in the phosphorylation status of molecules that could influence the
 202 interpretation of IL-3-mediated signaling. The only significant difference in steady-state
 203 phosphorylation was observed in rpS6^{Ser235/236} and STAT5^{Tyr694}, the former exhibiting a
 204 median fluorescence intensity (MFI) of 18.9 ± 1.1 in $MYB^{WT/WT}$ K11bL cells versus 52.5 ± 2.4
 205 ($p=0.003$) in $MYB^{KD/KD}$ cells and the latter being 26.4 ± 1.5 in $MYB^{WT/WT}$ compared to 47.9 ± 0.3
 206 ($p=0.0026$) in $MYB^{KD/KD}$ cells (**Supplementary Figure 3A**).

207 In order to assess the effect of IL-3 stimulation on the dynamics of phosphorylation, K11bL
 208 cells were starved of serum prior to stimulation with IL-3 and subsequent analysis 15 min
 209 later. We observed differences in both the extent of the response and the relative degree of
 210 phosphorylation of rpS6^{Ser235/236} and rpS6^{Ser240/244}. Hence, stimulation of K11bL cells with IL-3
 211 led to an increase in rpS6^{Ser235/236} phosphorylation, reflected in a MFI shift of 105 ± 36 to
 212 232 ± 32 ($p=0.009$) for $MYB^{WT/WT}$ and 91 ± 29 to 480 ± 82 ($p=0.0002$) for $MYB^{KD/KD}$ (**Figure 4Ai**
 213 **and Supplementary Figure 3B**). This also revealed that $MYB^{KD/KD}$ K11bL cells showed a

214 significantly greater increase in the proportion of cells phosphorylated at this site and
215 reached an overall higher level of phosphorylation, the MFI being twice as great as that seen
216 in *MYB^{WT/WT}* K11bL cells ($p=0.0063$; **Supplementary Figure 3B**). We therefore also
217 checked for changes in phosphorylation at the rpS6^{Ser240/244} site. Following IL-3 stimulation,
218 no significant increase in phosphorylation was seen in *MYB^{WT/WT}* K11bL cells, whereas
219 *MYB^{KD/KD}* K11bL cells demonstrated a small increase, seen as a shift in MFI of 13.3 ± 3 to
220 22.9 ± 4 ($p=0.02$) (**Figure 4Ai and Supplementary Figure 3C**).

221 Phosphorylation of rpS6^{Ser235/236} can occur through activation of the PI3k/AKT/mTOR or
222 RAS/MAPK pathways, whereas only the former leads to the modification of rpS6^{Ser240/244}
223 (11). We examined the phosphorylation status of AKT (Thr308 and Ser473) and p44/42
224 MAPK (ERK1/2) to investigate the relative use of the two pathways. At 15 min post IL-3
225 stimulation we failed to detect any phosphorylation of AKT or p44/42 MAPK (data not
226 shown). However, reasoning that the response to IL-3 might be very rapid, we also looked at
227 phosphorylation at 5 min following IL-3 addition. A significant increase in phosphorylation of
228 AKT^{Thr308} was seen as a shift in MFI from 6.7 ± 1.5 to 13.8 ± 4.5 ($p=0.047$) (**Figure 4Aii and**
229 **Supplementary Figure 3D**). We also observed an increase in the percentage of cells
230 positive for p44/42 MAPK phosphorylation from $4\pm 3\%$ to $23\pm 5\%$ ($p=0.04$) in *MYB^{KD/KD}* K11bL
231 cells but not in the *MYB^{WT/WT}* equivalent (**Figure Aii and Supplementary Figure 3E**).

232 To confirm the dependence of rpS6 phosphorylation on the PI3k/AKT/mTOR and
233 RAS/MAPK pathways and better to define how the specificity and balance of activity differs
234 in *MYB^{KD/KD}* K11bL cells compared to *MYB^{WT/WT}* cells, we performed IL-3 stimulations
235 following pre-treatment of the K11bL cells with inhibitors of mTOR (Rapamycin) or MEK
236 (U0126). Treatment of *MYB^{WT/WT}* cells with Rapamycin but not U0126 resulted in a loss of
237 phosphorylation of rpS6^{Ser235/236} from $21.8\pm 3.2\%$ to $12.5\pm 2.7\%$ ($p=0.02$, **Supplementary**
238 **Figure 3F**). Similar analysis of rpS6 in *MYB^{KD/KD}* K11bL cells showed that phosphorylation at
239 Ser235/236 was inhibited by U0126 ($45.5\pm 7.1\%$ to $13.7\pm 3.5\%$; $p=9.5\times 10^{-05}$) but not by
240 Rapamycin, whereas the Ser240/244 site modification was susceptible to inhibition of mTOR

241 but not MEK (**Figure 4B and Supplementary Figure 3F**). This implies that one aspect of
242 the distinctive cytokine responsiveness seen in *MYB^{KD/KD}* K11bL cells relates to a shift in the
243 relative usage of the signaling pathways downstream of the IL-3 receptor.

244 The baseline phosphorylation of STAT5^{Tyr694} was lower in *MYB^{KD/KD}* K11bL cells but upon
245 stimulation with IL-3 increased to a level similar to that seen in *MYB^{WT/WT}* cells following their
246 treatment with cytokine (**Figure 4Ci**). Consistent with the phosphorylation of STAT5 being
247 elicited through a JAK protein, we observed no effect on the level of phosphorylation in the
248 presence of the mTOR or MEK inhibitors (**Figure 4Cii**).

249 **The expression of signaling-associated genes defines the *MYB^{KD/KD}* K11bL phenotype**

250 Based on the phosphorylation results, we further analysed the array data to look at GO
251 groups associated with signaling. Analysis of deregulated genes involved in intracellular
252 signal transduction (GO:1902532) (**Supplementary Table 8**) and in particular proteins
253 involved in the ERK signalling cascade (GO:0070372) (**Supplementary Table 9**) highlighted
254 the altered expression of several genes. In particular, we noted that *MYB^{KD/KD}* K11bL cells
255 exhibit lower expression of the genes encoding the inhibitor SPROUTY2 (*SPRY2*), the dual
256 specificity phosphatase 6 (*DUSP6*), and the RAS protein activator (*RASA2*), and higher
257 expression of dual specificity phosphatase 3 (*DUSP3*), and suppressor of cytokine signalling
258 3 (*SOCS3*).

259 In order to confirm which of these differences might reflect direct regulation by MYB we used
260 our conditional *MYB* knockout (12). K11bL cells were isolated from control mice
261 (*MYB^{+/+}:Cre*) and *MYB* knockout (*MYB^{F/F}:Cre*) mice 24 hours after induction of deletion, and
262 the levels of RNA for *MYB* and the selected genes were measured by quantitative RT-PCR.
263 This confirmed that *SPRY2* and *DUSP6* RNA levels were depleted, whilst the levels of
264 *IL3RA*, *CSF2RB*, *CSFR2RB2*, *CSFR1*, *SOCS3*, *DUSP3*, *MECOM*, and *CCND1* were higher,
265 suggesting that the expression of these genes could be directly inhibited by MYB (**Figure**
266 **5A**).

267 **MYB directly regulates expression of the *SPRY2* and *DUSP6* genes**

268 We next used X-ChIP to determine if positive regulation of the *SPRY2* and *DUSP6* genes by
269 MYB correlates with binding of the protein to gene regulatory regions. We prepared
270 chromatin from the murine HSC line HPC-7 (13), and used an antibody against MYB for
271 immunoprecipitation of *SPRY2* and *DUSP6* gene fragments corresponding to *in vivo* binding
272 sites for the factor. Primers for quantitative PCR were designed around highly conserved
273 regions that contained potential MYB binding sequences. In this way, we demonstrated MYB
274 binding to the *SPRY2* promoter (-0.55kb from ATG, **Figure 5B**) and the *DUSP6* promoter (-
275 2.7kb from ATG, **Figure 5C**), whereas there was no significant enrichment of either the
276 *SPRY2* enhancer (-26kb from ATG) or the *DUSP6* distal promoter (-2.7kb from ATG)
277 (**Supplementary Figure 4**).

278 **Reduced MYB expression in human progenitors mirrors the changes seen in *MYB*^{KD/KD}**
279 **K11bL cells**

280 To examine if our observations in the mouse system are paralleled in human cells we
281 transfected CD34+ cord blood cells with *MYB* siRNA. This achieved a 50% reduction in
282 *MYB* gene expression at 24 hours, and upon plating cells in methylcellulose containing
283 myeloid growth factors we observed that knockdown of MYB leads to an increase in CFU-M
284 and CFU-Mk and a reduction in CFU-G, CFU-GEMM and BFU-E, in line with the broad
285 phenotypic changes seen in *MYB*^{KD/KD} K11bL cells (**Figure 6A**). We also showed that the
286 knockdown of MYB in the human cells led to a significant decrease in the expression of
287 *SPRY2* and increased expression of *IL3RA* and *CSF1R*, exactly as we saw in murine
288 *MYB*^{KD/KD} K11bL cells, however, unlike in mouse K11bL cells, the expression of *DUSP6* was
289 significantly increased (**Figure 6B**).

290 **Manipulation of *SPRY2* expression in *MYB*^{WT/WT} cells partially recapitulates the**
291 ***MYB*^{KD/KD} stem cell phenotype**

292 Based on the apparent importance of enhanced IL-3-dependent RAS/MAPK signaling in
293 *MYB^{KD/KD}* K11bL cells and the conserved MYB-dependent expression of *SPRY2* in both
294 mouse and human progenitor cells, we reasoned that *SPRY2* is pivotal to the way in which
295 IL-3 can influence stem cell characteristics of myeloid progenitors. In order to assess the
296 degree to which *SPRY2* is responsible for the gain of stem cell function, we transduced
297 *MYB^{WT/WT}* K11bL cells with a lentiviral vector expressing shRNA directed against *SPRY2* and
298 assayed their ability to form hematopoietic colonies *in vitro*. *MYB^{WT/WT}* K11bL cells
299 transduced with control virus demonstrated normal colony formation in complete
300 methylcellulose. In contrast, *MYB^{WT/WT}* cells transduced with lentivirus expressing *SPRY2*
301 shRNA (which exhibited >95% knockdown - **Supplementary Figure 5A**) demonstrated
302 reduced CFU-G colonies and increased CFU-M colonies, similar to the situation seen for
303 *MYB^{KD/KD}* K11bL cells (**Figure 7A**). Secondary plating of *MYB^{WT/WT}* K11bL cells experiencing
304 *SPRY2* knockdown resulted in colonies that covered the plate, whereas control cells formed
305 very small, sparsely distributed colonies (**Supplementary Figure 5B**). These *SPRY2*
306 knockdown *MYB^{WT/WT}* K11bL secondary colonies showed increased levels of KIT and CD34
307 compared to the control cells (**Supplementary Figure 5C**).

308 Transplantation assays of *MYB^{WT/WT}* K11bL cells transduced with control or *SPRY2* shRNA
309 revealed a higher donor to reference ratio when levels of *SPRY2* were reduced (**Figure 7B**).
310 This enhanced engraftment was further amplified by 3 months but the contribution to
311 peripheral myeloid cells (CD11b+) was not altered (**Supplementary Figure 5D**). Secondary
312 transplantation revealed the acquisition of long-term repopulating ability by the *SPRY2*
313 knockdown K11bL cells (**Supplementary Figure 5E**). We then asked if over expression of
314 *SPRY2* in *MYB^{KD/KD}* K11bL cells could reverse their proliferation and differentiation
315 characteristics. Colony forming assays of *MYB^{KD/KD}* K11bL cells transduced with a lentivirus
316 expressing *SPRY2* resulted in a significant reduction in colony number in complete
317 methylcellulose (**Figure 7C**). Additionally the *SPRY2*-overexpressing *MYB^{KD/KD}* K11bL cells

318 gave rise to a lower proportion of megakaryocyte colonies and increased granulocytic
319 colonies compared to K11bL cells infected with control virus (**Figure 7C**).

320

321 **DISCUSSION**

322 MYB was originally shown to be a critical regulator of hematopoiesis since complete ablation
323 abolished definitive hematopoiesis (14). The role that MYB plays in adult hematopoiesis has
324 been studied using mouse models with reduced activity of the protein (5, 6, 12, 15),
325 revealing a role for MYB in immature proliferating hematopoietic cells. Here we have sought
326 to link recent observations on the genetic predisposition to MPN caused by lower levels of
327 expression of MYB (4) with the phenotype seen in our mouse model for decreased MYB
328 activity. We show that lower MYB levels in myeloid progenitors results in; (i) altered short-
329 term homing towards the spleen, (ii) differentiation towards myelomonocytic cells, and (iii) a
330 stem cell phenotype, including self-renewal potential that is not seen in the normal
331 equivalents and giving a phenotype more similar to those described in some chronic myeloid
332 leukemia (CML) and acute promyelocytic leukemia (APL) stem cells (16, 17).

333 Key to the *MYB^{KD/KD}* phenotype is altered IL-3 signaling, particularly along the RAS/MAPK
334 pathway. Our results suggest that enhanced IL-3 signaling is responsible for aspects of the
335 aberrant stem cell phenotype, including homing to the spleen, engraftment potential, and
336 lineage bias. Such acquired properties likely have relevance to the leukemia stem cell-
337 specific role of IL-3 receptor in acute myeloid leukemia (AML), which has been shown to be
338 an effective target for an anti-IL3RA (CD123) antibody (18).

339 We are presently investigating the mechanisms by which increased IL-3-dependent signaling
340 leads to the *MYB^{KD/KD}* phenotype. The RAS/MAPK pathway appears to be central and,
341 although the nature of the critical targets remains unclear, we found evidence for the
342 activation of ribosomal protein S6, which itself plays an essential role in protein translation of
343 several pro-survival protein genes such as MYC, BCL-XL, and SURVIVIN, and might

344 therefore contribute to the gain of stem cell properties. Interestingly, there are descriptions of
345 the importance of ERK/MAPK in self-renewal of both embryonic and adult stem cells (19,
346 20). The RAS/MAPK pathway is frequently activated in hematological malignancy and has
347 been implicated in the sensitivity and resistance of cells to therapy (21), including in other
348 MPN models such as the KRAS mutant mouse (22).

349 We explored the mechanisms by which reduced MYB activity leads to enhanced IL-3
350 signaling, and found that these involved multiple direct and indirect targets, and including
351 both positively and negatively regulated genes. Aside from what appears to be coordinated
352 positive regulation of several cytokine receptor genes, MYB also normally seems to provide
353 a coordinated controlling influence on RAS/MAPK signaling by promoting the expression of
354 negative pathway regulators, including SPRY2 and DUSP6. SPRY2, which prevents the
355 interaction between RAS and GRB2-SOS (23) following their recruitment by SHC when it
356 associates with the IL-3 receptor, seems to be relevant in both the mouse and human
357 systems we examined. The lower expression of SPRY2 would be expected to release the
358 inhibition of RAS, leading to an increased sensitivity to IL-3. Interestingly, knockdown of
359 *SPRY2* in wild type progenitor cells both shifted their phenotype and enhanced engraftment
360 potential, partially reflecting the overall phenotype of the *MYB^{KD/KD}* cells.

361 We postulate a working model for the signaling pathways utilized in K11bL cells in both
362 *MYB^{WT/WT}* and *MYB^{KD/KD}* mice (Figure 8), and clearly our study has opened up a whole new
363 chapter in the understanding of the pivotal role of MYB in both normal and malignant
364 hematopoiesis. Although numerous additional mechanisms undoubtedly combine to give rise
365 to the complete *MYB^{KD/KD}* MPN-like phenotype, our findings suggest that IL-3-dependent
366 signaling plays a major role, affecting the regulation of genes responsible for migration,
367 proliferation, and differentiation. For those hematological disorders where MYB activity is
368 affected, including MPN, the knowledge that signaling downstream of IL-3 receptor is
369 affected as a direct result of altered MYB levels could open up the possibility for a more
370 direct approach to treatment.

371

372 **ACKNOWLEDGMENTS**

373 This work was supported entirely by Bloodwise.

374

375 **CONFLICTS OF INTEREST**

376 The authors declare no conflicts of interest.

377 Supplementary information is available at <http://www.nature.com/leu/index.html>

378

379

380 REFERENCES

- 381 1. Campbell PJ, Green AR. The myeloproliferative disorders. *N Engl J Med*. 2006;355(23):2452-
382 66.
- 383 2. Klampfl T, Gisslinger H, Harutyunyan AS, Nivarthi H, Rumi E, Milosevic JD, et al. Somatic
384 mutations of calreticulin in myeloproliferative neoplasms. *N Engl J Med*. 2013;369(25):2379-90.
- 385 3. Pardanani AD, Levine RL, Lasho T, Pikman Y, Mesa RA, Wadleigh M, et al. MPL515 mutations
386 in myeloproliferative and other myeloid disorders: a study of 1182 patients. *Blood*.
387 2006;108(10):3472-6.
- 388 4. Tapper W, Jones AV, Kralovics R, Harutyunyan AS, Zoi K, Leung W, et al. Genetic variation at
389 MECOM, TERT, JAK2 and HBS1L-MYB predisposes to myeloproliferative neoplasms. *Nat Commun*.
390 2015;6:6691.
- 391 5. Garcia P, Clarke M, Vegiopoulos A, Berlanga O, Camelo A, Lorvellec M, et al. Reduced c-Myb
392 activity compromises HSCs and leads to a myeloproliferation with a novel stem cell basis. *EMBO J*.
393 2009;28(10):1492-504.
- 394 6. Lieu YK, Reddy EP. Conditional c-myb knockout in adult hematopoietic stem cells leads to
395 loss of self-renewal due to impaired proliferation and accelerated differentiation. *Proc Natl Acad Sci*
396 *U S A*. 2009;106(51):21689-94.
- 397 7. Clarke M, Dumon S, Ward C, Jager R, Freeman S, Dawood B, et al. MYBL2 haploinsufficiency
398 increases susceptibility to age-related haematopoietic neoplasia. *Leukemia*. 2013;27(3):661-70.
- 399 8. Krutzik PO, Nolan GP. Intracellular phospho-protein staining techniques for flow cytometry:
400 monitoring single cell signaling events. *Cytometry A*. 2003;55(2):61-70.
- 401 9. Sommer CA, Stadtfeld M, Murphy GJ, Hochedlinger K, Kotton DN, Mostoslavsky G. Induced
402 pluripotent stem cell generation using a single lentiviral stem cell cassette. *Stem Cells*.
403 2009;27(3):543-9.
- 404 10. Dumon S, Walton DS, Volpe G, Wilson N, Dasse E, Del Pozzo W, et al. Itga2b regulation at the
405 onset of definitive hematopoiesis and commitment to differentiation. *PLoS One*. 2012;7(8):e43300.
- 406 11. Roux PP, Shahbazian D, Vu H, Holz MK, Cohen MS, Taunton J, et al. RAS/ERK signaling
407 promotes site-specific ribosomal protein S6 phosphorylation via RSK and stimulates cap-dependent
408 translation. *J Biol Chem*. 2007;282(19):14056-64.
- 409 12. Emambokus N, Vegiopoulos A, Harman B, Jenkinson E, Anderson G, Frampton J. Progression
410 through key stages of haemopoiesis is dependent on distinct threshold levels of c-Myb. *EMBO J*.
411 2003;22(17):4478-88.
- 412 13. Pinto do OP, Kolterud A, Carlsson L. Expression of the LIM-homeobox gene LH2 generates
413 immortalized steel factor-dependent multipotent hematopoietic precursors. *EMBO J*.
414 1998;17(19):5744-56.
- 415 14. Mucenski ML, McLain K, Kier AB, Swerdlow SH, Schreiner CM, Miller TA, et al. A functional c-
416 myb gene is required for normal murine fetal hepatic hematopoiesis. *Cell*. 1991;65(4):677-89.
- 417 15. Sandberg ML, Sutton SE, Pletcher MT, Wiltshire T, Tarantino LM, Hogenesch JB, et al. c-Myb
418 and p300 regulate hematopoietic stem cell proliferation and differentiation. *Dev Cell*. 2005;8(2):153-
419 66.
- 420 16. Guibal FC, Alberich-Jorda M, Hirai H, Ebralidze A, Levantini E, Di Ruscio A, et al. Identification
421 of a myeloid committed progenitor as the cancer-initiating cell in acute promyelocytic leukemia.
422 *Blood*. 2009;114(27):5415-25.
- 423 17. Bruns I, Czibere A, Fischer JC, Roels F, Cadeddu RP, Buest S, et al. The hematopoietic stem
424 cell in chronic phase CML is characterized by a transcriptional profile resembling normal myeloid
425 progenitor cells and reflecting loss of quiescence. *Leukemia*. 2009;23(5):892-9.
- 426 18. Jin L, Lee EM, Ramshaw HS, Busfield SJ, Peoppl AG, Wilkinson L, et al. Monoclonal antibody-
427 mediated targeting of CD123, IL-3 receptor alpha chain, eliminates human acute myeloid leukemic
428 stem cells. *Cell Stem Cell*. 2009;5(1):31-42.

- 429 19. Chen H, Guo R, Zhang Q, Guo H, Yang M, Wu Z, et al. Erk signaling is indispensable for
430 genomic stability and self-renewal of mouse embryonic stem cells. *Proc Natl Acad Sci U S A*.
431 2015;112(44):E5936-43.
- 432 20. Geest CR, Coffey PJ. MAPK signaling pathways in the regulation of hematopoiesis. *J Leukoc*
433 *Biol*. 2009;86(2):237-50.
- 434 21. Malumbres M, Barbacid M. RAS oncogenes: the first 30 years. *Nat Rev Cancer*.
435 2003;3(6):459-65.
- 436 22. Lyubynska N, Gorman MF, Lauchle JO, Hong WX, Akutagawa JK, Shannon K, et al. A MEK
437 inhibitor abrogates myeloproliferative disease in Kras mutant mice. *Sci Transl Med*.
438 2011;3(76):76ra27.
- 439 23. Yusoff P, Lao DH, Ong SH, Wong ES, Lim J, Lo TL, et al. Sprouty2 inhibits the Ras/MAP kinase
440 pathway by inhibiting the activation of Raf. *J Biol Chem*. 2002;277(5):3195-201.
- 441 24. Bolstad BM, Irizarry RA, Astrand M, Speed TP. A comparison of normalization methods for
442 high density oligonucleotide array data based on variance and bias. *Bioinformatics*. 2003;19(2):185-
443 93.
- 444 25. Irizarry RA, Bolstad BM, Collin F, Cope LM, Hobbs B, Speed TP. Summaries of Affymetrix
445 GeneChip probe level data. *Nucleic Acids Res*. 2003;31(4):e15.
- 446 26. Smyth GK. Linear models and empirical bayes methods for assessing differential expression
447 in microarray experiments. *Stat Appl Genet Mol Biol*. 2004;3:Article3.

448

449 SUPPLEMENTARY METHODS**450 Bone marrow cell isolation and culture**

451 All mice were maintained on a C57/BL6 background and sacrificed at 4 weeks of age as a
452 source of bone marrow. Conditional deletion of *MYB* was induced by intraperitoneal injection
453 of 250µg poly(inosinic-cytidylic) acid (pIpC, Sigma) and 24 hours later were sacrificed for
454 bone marrow analysis. Peripheral blood was collected from the tail vein into acid citrate
455 dextrose (ACD) solution. Sorted mouse K11bL cells were plated in complete methylcellulose
456 medium (Methocult M3434, Stem Cell Technologies) containing TPO (25ng/ml). Methocult
457 lacking growth factors (M3234) was used to assess the response to specific cytokines.

458 Homing assays

459 For live animal imaging, mice were shaved and imaged using an IVIS spectrum under 2.5%
460 iso-fluorane (Caliper Life Sciences). Mice were imaged ventrally at 1 and 24 hours. Images
461 were acquired by trans-illumination at 745nm excitation and 800nm emission with exposure
462 times ranging from 1.4 seconds to 60 seconds, medium binning and f-stop 2. IVIS data was
463 analysed using Living Image 4.0 software (Caliper Life Sciences).

464 Gene expression analysis

465 Scanned images of microarrays were analyzed using the Affymetrix GeneChip Command
466 Console. Probe level quantile normalization (24) and robust multi-array analysis (25) on the
467 raw CEL files were performed using Affymetrix Expression Console. Differentially expressed
468 genes were identified using limma with absolute fold change >1.5 and $p < 0.01$ (26). Gene
469 ontology was analysed using Gene Ontology Enrichment Analysis Software Toolkit
470 (GOEAST).

471

472 **FIGURE LEGENDS**

473 **Figure 1** A) Whole bone marrow cells were gated for expression of KIT and CD11b and then
 474 analysed for expression of lineage markers **** $p \leq 0.0001$. B) Primary donor-derived cells in
 475 the peripheral blood analyzed for expression of myeloid, B-cell, and T-cell markers at 3
 476 months post-transplantation. Numbers represent average percentage of total cells. C)
 477 Representative (N=10) flow cytometry profiles of $MYB^{WT/WT}$ (black) and $MYB^{KD/KD}$ (red)
 478 K11bL cells (isotype control - solid grey).

479 **Figure 2** A) Quantitative RT-PCR analysis of RNA expression for the indicated genes in
 480 K11bL cells (N=3). B) 500 sorted K11bL cells from $MYB^{WT/WT}$ and $MYB^{KD/KD}$ mice were
 481 plated in methylcellulose with varying concentrations of IL3. Colony number was scored after
 482 7 days (N=2). C) Colony morphology of K11bL cells plated in M3234 containing 20ng/ml IL-
 483 3. Inset: i) Representative images of $MYB^{WT/WT}$ CFU-G (left), CFU-GM (middle), and CFU-M
 484 (right) colonies, and ii) $MYB^{KD/KD}$ CFU-M colonies

485 **Figure 3** A) Sorted K11bL cells were incubated in the presence of 30 μ g/ml of isotype or anti-
 486 IL3RB neutralizing antibody prior to plating in complete methylcellulose. Colony number was
 487 assayed after 7 days (** $p \leq 0.01$ N=3). B) $MYB^{KD/KD}$ K11bL cells were transduced with
 488 lentivirus carrying shRNA control or shRNA *Ii3ra* before being injected into lethally irradiated
 489 mice: i) Transduced cells remaining in culture were assessed for transduction efficiency by
 490 GFP expression; ii) Peripheral blood from recipient mice was analyzed at 1 and 3 months
 491 post-transplantation to assess engraftment, the gates showing the CD45.2+ donor cells with
 492 the respective average reference:donor ratios. C) Staining with DiR and injection into lethally
 493 irradiated B6:SJL recipient mice. Recipients were imaged by IVIS after 24 hours by trans-
 494 illumination. The oval region highlighted indicates the region of the spleen measured.
 495 Images are representative of N=4.

496 **Figure 4.** Representative plots depicting phospho-flow analysis of K11bL cells, and the
 497 response to IL-3 stimulation. A) K11bL cells were serum-starved (solid black/red) prior to
 498 stimulation with 20ng/ml IL-3 (dashed black/red) for 15 min and then fixed and permeabilized

499 before staining with antibodies against i) phospho-rpS6^{Ser235/236} and phospho-rpS6^{Ser240/244}
 500 (N=9). And ii) phospho-AKT^{Thr308}, phospho-AKT^{Ser473} and phospho-p44/42 MAPK following
 501 IL-3 stimulation (N=3). (isotype control – pale grey) B) *MYB*^{KD/KD} K11bL cells were incubated
 502 with IL-3 in the presence and absence of mTOR inhibitor Rapamycin (1μM, red) or the MEK
 503 inhibitor U0126 (10μM, blue) (N=3). C) Staining of K11bL cells for P-Stat5^{Y694} following i)
 504 serum starvation (solid black/red) and stimulation with IL3 (dashed black/red) and ii) following
 505 stimulation with IL3 in the presence of either Rapamycin (red) or U0126 (blue).

506 **Figure 5** A) K11bL cells from *MYB*^{+/+}:*Cre* and *MYB*^{FF}:*Cre* bone marrow were sorted 24 hours
 507 following intraperitoneal injection of plpC to induce *Myb* gene deletion. Expression of the
 508 indicated signaling-associated genes was analyzed by quantitative RT-PCR and normalized
 509 against *β2M*. Error bars represent SEM (N=3). B) Alignment of mammalian sequences for
 510 the *SPRY2* gene, showing the gene exonic structures, the presence of CpG islands, the
 511 overall degree of sequence conservation, and the detail of the sequence conservation
 512 around potential MYB binding sites (red box) that were spanned by the Q-PCR primers. The
 513 histogram shows the results of quantitative PCR performed on HPC7 ChIP samples pulled
 514 down by MYB antibody and analysed for enrichment of binding on sequences for *SPRY2*.
 515 The histogram illustrates the relative enrichment as determined by Q-PCR (N=3,
 516 ***p≤0.001). C) A similar analysis to that described in (B) for the *DUSP6* gene.

517 **Figure 6** A) Human CD34+ cells were isolated from human umbilical cord blood by FACS
 518 and transfected with either siRNA control or siRNA *MYB* and after 24 hours FAM+ cells were
 519 plated in complete methylcellulose and assayed for their ability to undergo full myeloid
 520 differentiation after 10 days in culture. B) Cells were also collected at 24 hours for the
 521 preparation and analysis of RNA expression. The histograms illustrate quantitative RT-PCR
 522 measurements of RNA expression for the *MYB*, *SPRY2*, *DUSP3*, *DUSP6*, *IL3RA* and
 523 *CSF1R* genes ** p≤0.001, **** p≤0.0001.

524 **Figure 7** A) *MYB*^{WT/WT} K11bL cells were transduced with shRNA *SPRY2* and a
 525 corresponding shRNA control and 24 hours later were sorted on the basis of GFP

526 expression and plated in complete methylcellulose. After 7 days in culture colonies were
527 counted and their size scored GM: granulocyte / macrophage, G: Granulocyte, M:
528 Macrophage, Mixed: containing all types. (N=3). B) *MYB^{WT/WT}* K11bL cells were transduced
529 with shRNA *SPRY2* and transplanted into lethally irradiated recipients. Peripheral blood was
530 sampled monthly and the ratio of test donor to reference cells was determined. C)
531 Overexpression of *SPRY2* in *MYB^{KD/KD}* K11bL cells followed by plating in complete
532 methylcellulose (*p≤0.05) showing both colony number and myeloid differentiation potential
533 in control and *SPRY2* over expressing *MYB^{KD/KD}* K11bL cells.

534 **Figure 8 Working model of pathway utilization in *MYB^{WT/WT}* and *MYB^{KD/KD}* K11bL cells.**

535 Schematic representation of IL-3 receptor signaling in K11bL cells, illustrating the differences
536 in rpS6 phosphorylation observed in *MYB^{WT/WT}* versus *MYB^{KD/KD}* cells and how this appears
537 to relate to changes in the signaling pathways utilized and the MYB-regulated signaling
538 modulator *SPRY2*. The thickness of the arrows and the representation of the rpS6
539 phosphorylation sites gives a relative indication of the extent of pathway involvement and
540 how this differs between the *MYB^{WT/WT}* and *MYB^{KD/KD}* cells.

541

542

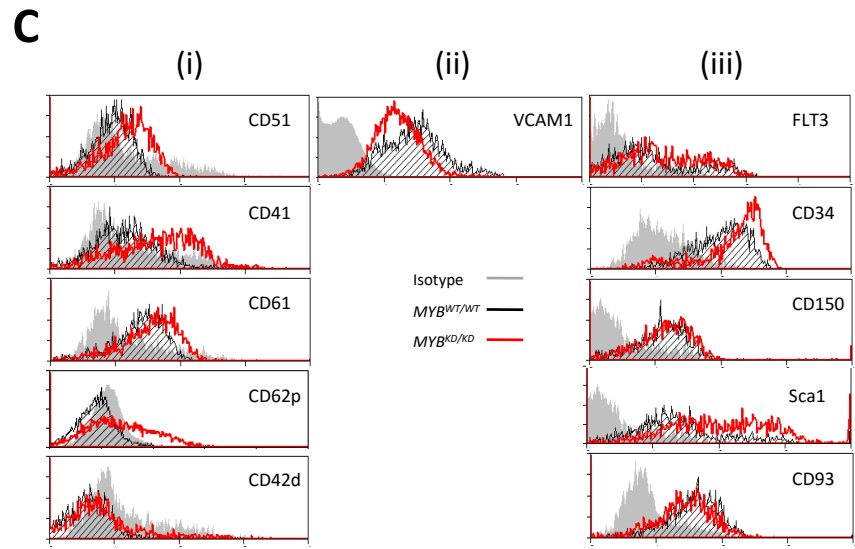
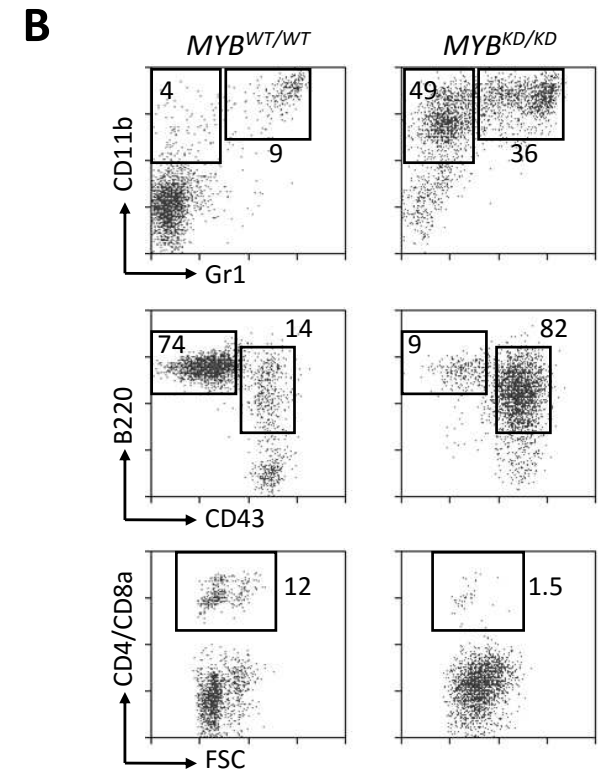
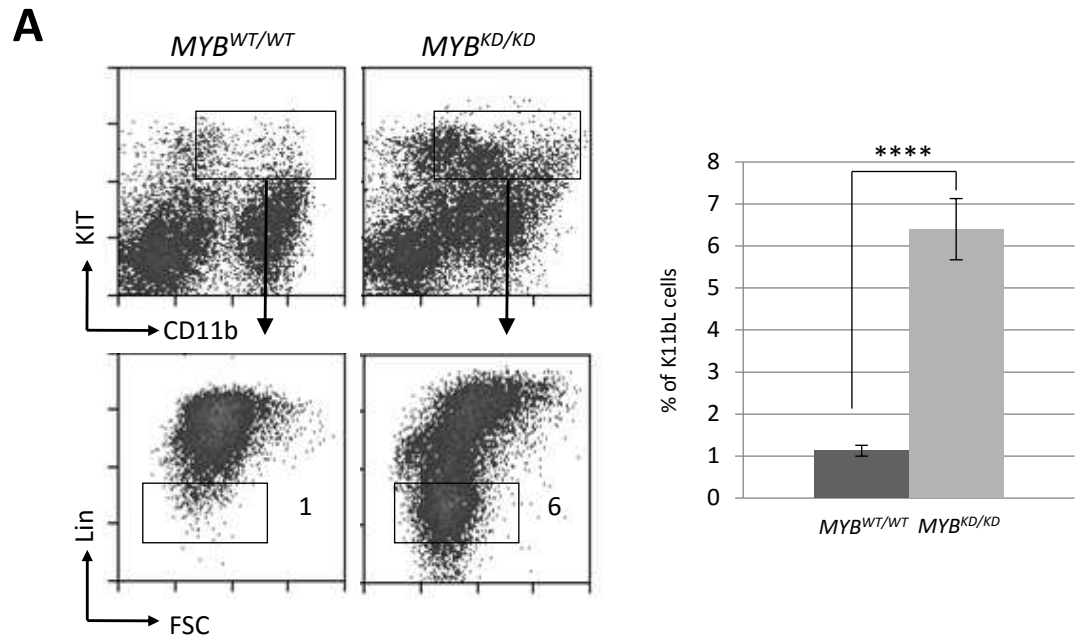


Figure 1

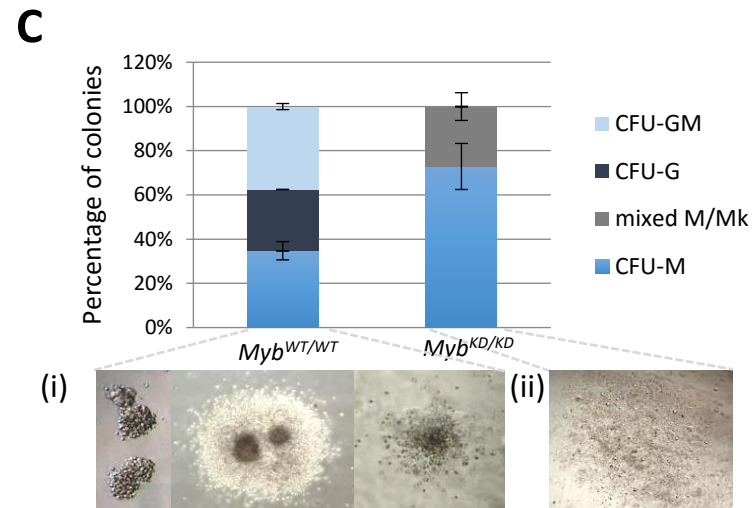
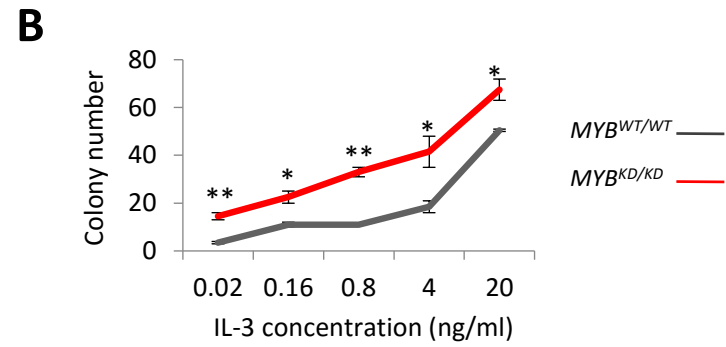
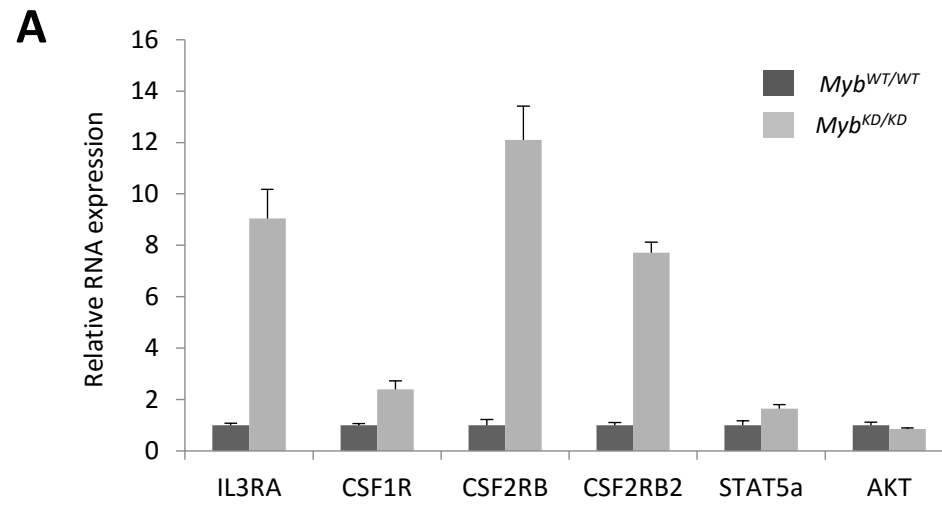
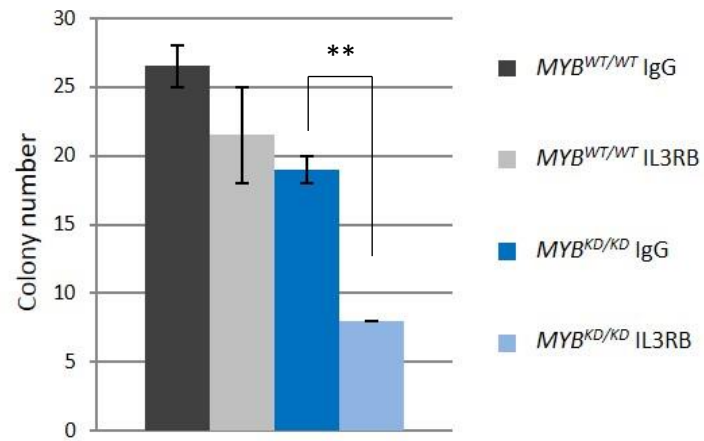
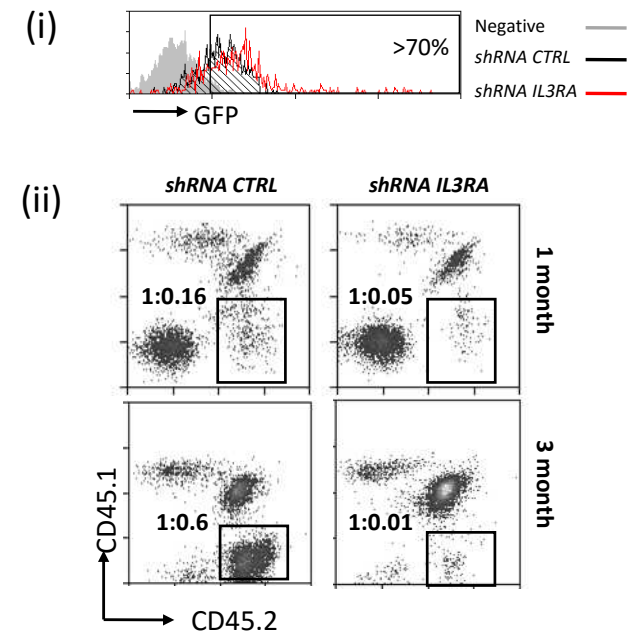
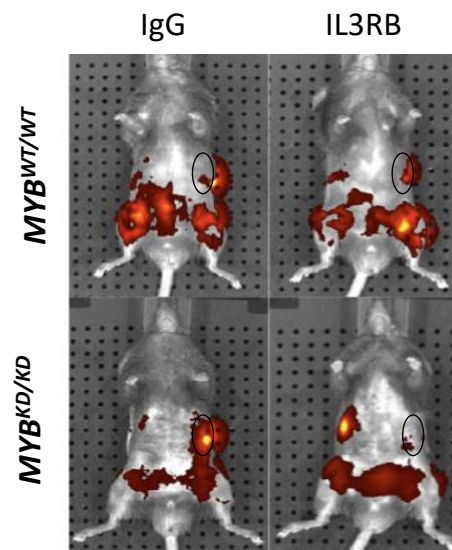


Figure 2

A**B****C****Figure 3**

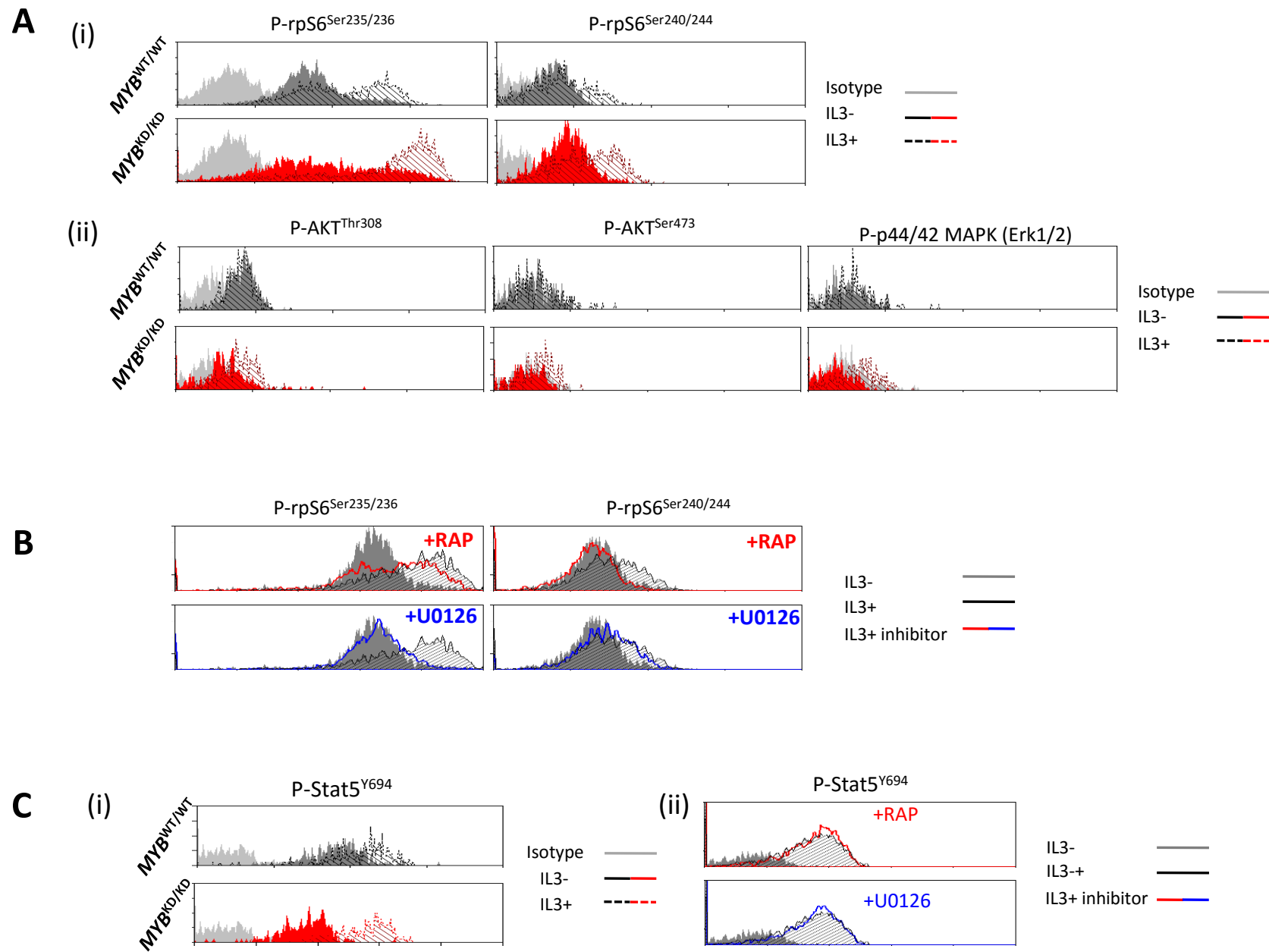


Figure 4

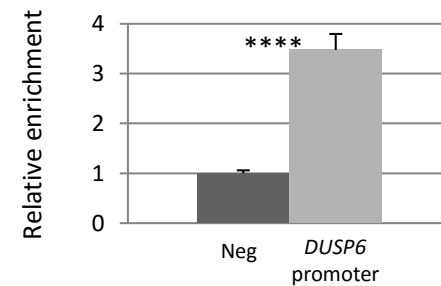
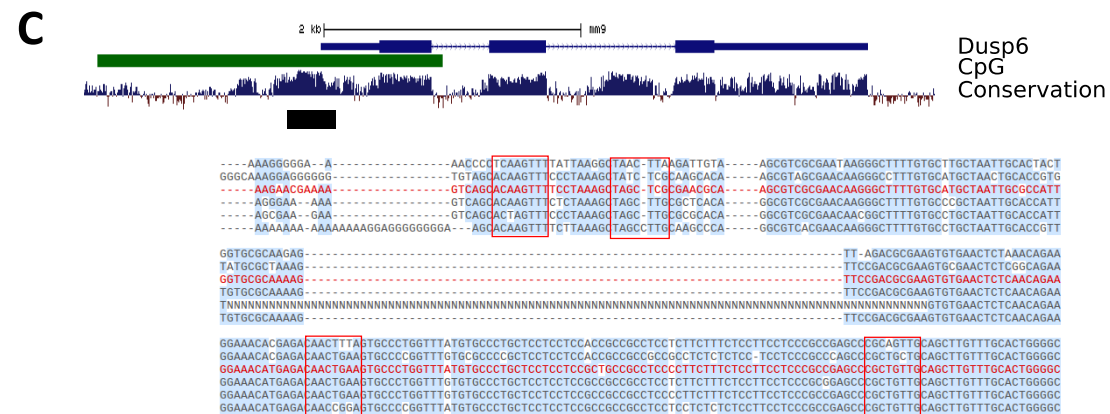
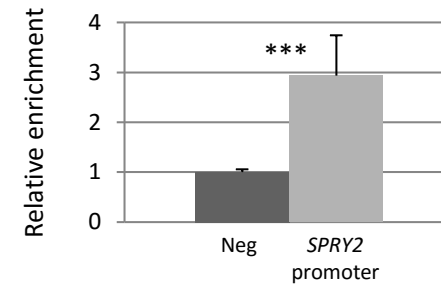
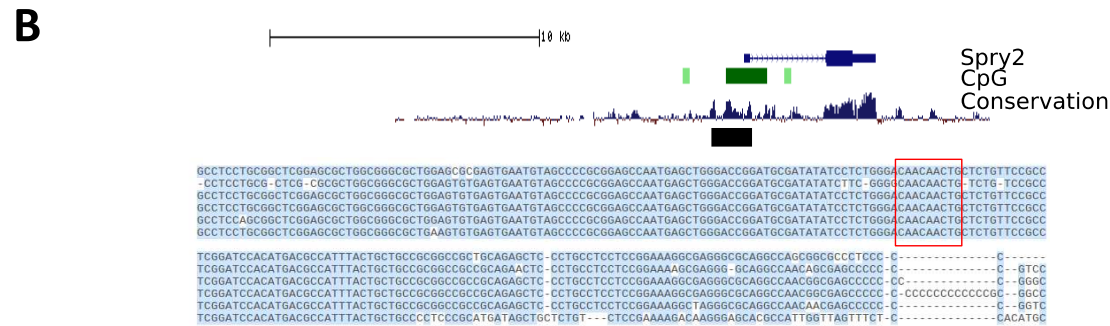
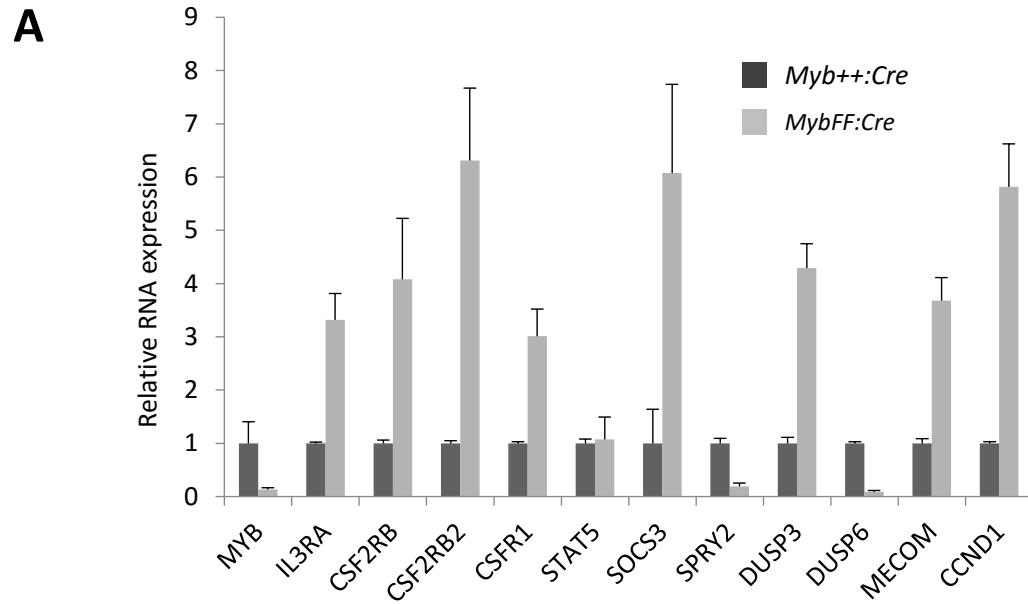
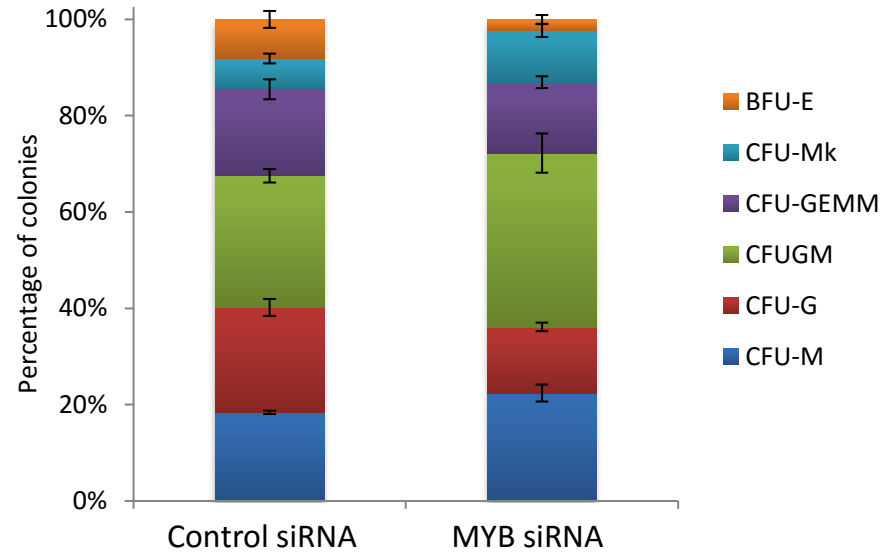
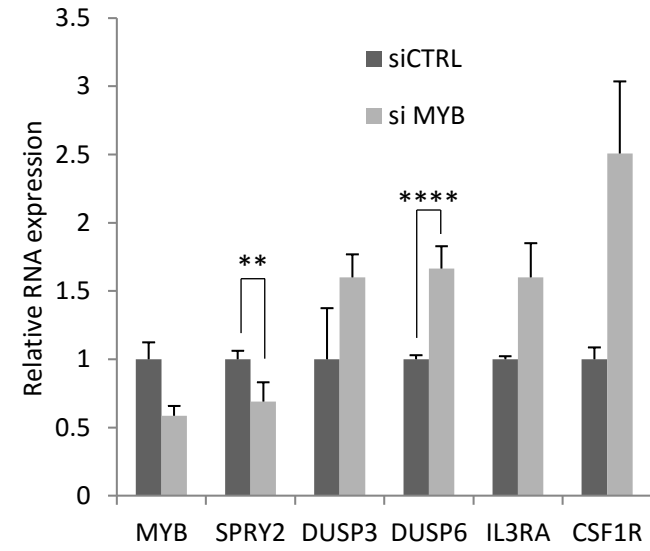
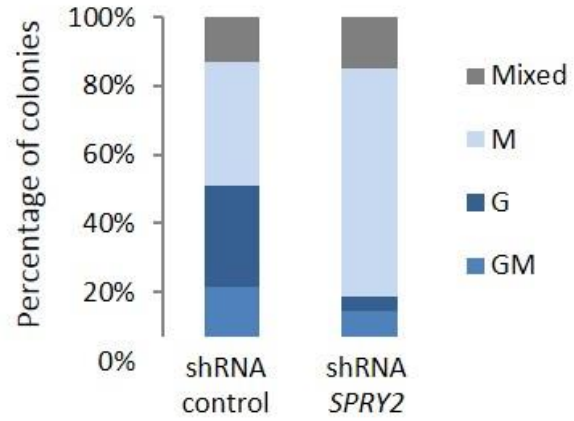
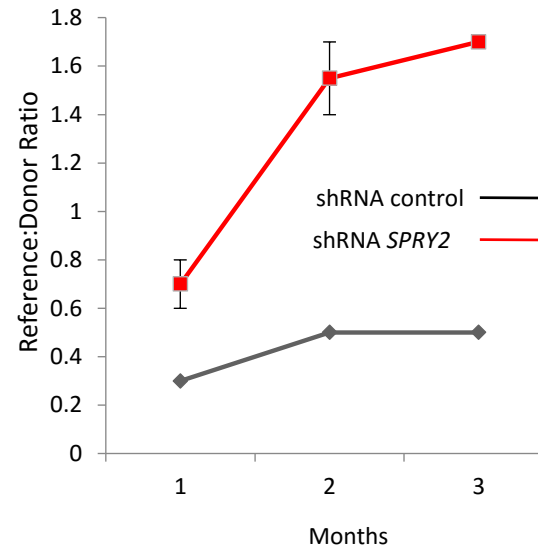
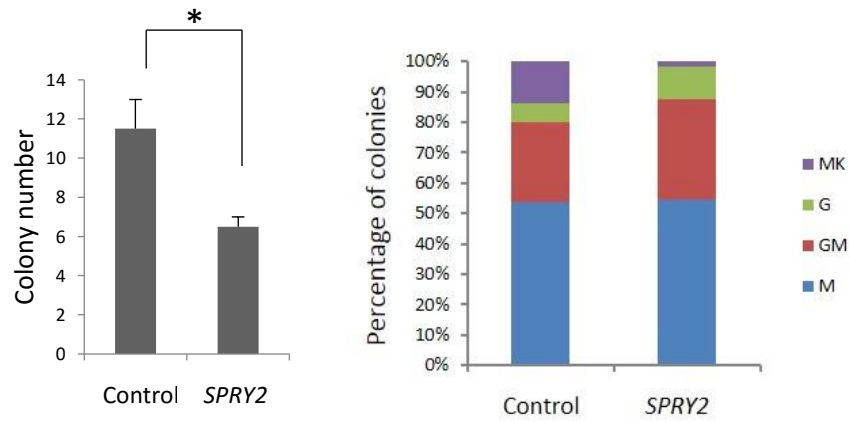
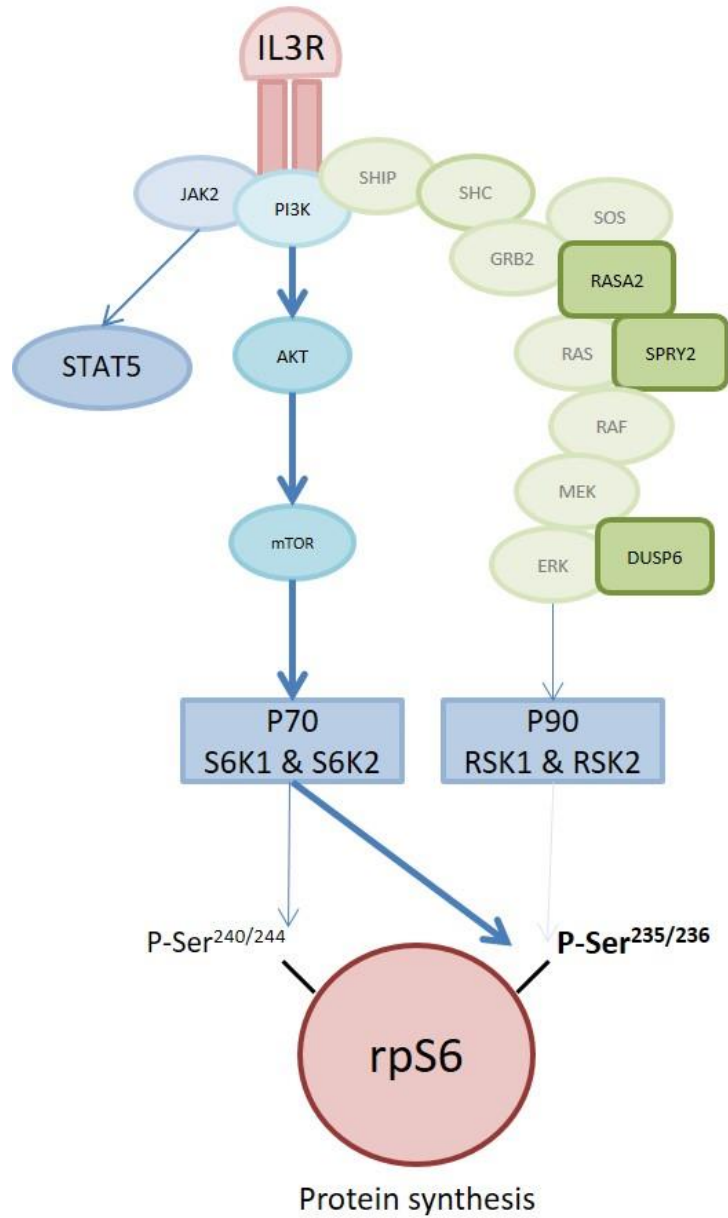


Figure 5

A**B****Figure 6**

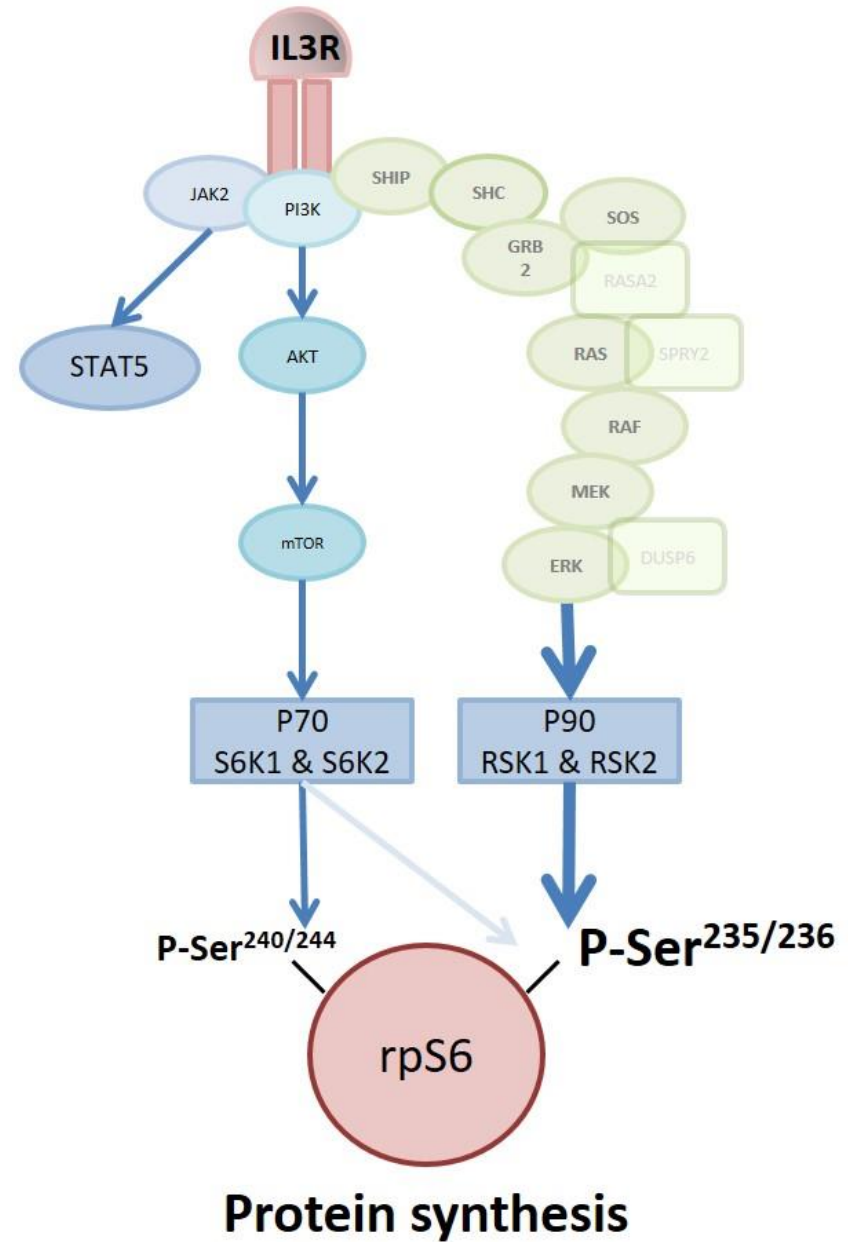
A**B****C****Figure 7**

MYB^{WT/WT} K11bL cells



Regulated cell proliferation, cell size and apoptosis

MYB^{KD/KD} K11bL cells



Enhanced cell proliferation, cell size and survival

Figure 8